Hindawi Publishing Corporation
EURASIP Journal on Advances in Signal Processing
Volume 2008, Article ID 378092, 8 pages
doi:10.1155/2008/378092

Research Article

Selective Weighting of Undecimated Wavelet Coefficients for Noise Reduction in SAR Interferograms

Vidhyasaharan Sethu,[1] Eliathamby Ambikairajah,[1] and Linlin Ge[2]

[1] *School of Electrical Engineering and Telecommunications, The University of New South Wales, Sydney, NSW 2052, Australia*
[2] *School of Surveying and Spatial Information Systems, The University of New South Wales, Sydney, NSW 2052, Australia*

Correspondence should be addressed to Vidhyasaharan Sethu, vidhyasaharan@gmail.com

Received 2 January 2007; Revised 10 October 2007; Accepted 13 February 2008

Recommended by A. Enis Çetin

This paper describes a technique for noise reduction in synthetic aperture radar interferometry. The noisy interferogram is decomposed using undecimated wavelet transform and the coefficients are weighted. A novel method for computing the weights for each subband, based on an estimate of the relative noise content in them, is presented with a median filter used as the noise estimator. The proposed technique is not optimised for any specific signal or noise models. Results show that this technique provides an improvement of around 15% over the conventional boxcar filter in terms of estimated height error of a digital elevation model constructed from the filtered interferogram.

1. INTRODUCTION

Synthetic aperture radar interferometry (InSAR) is an established technique for the extraction of height information by using SAR remote sensing [1]. It uses two high-resolution complex SAR images of the same scene to generate an interferogram. The phase information contained in this interferogram is extracted to generate a digital elevation model (DEM). As this phase information is wrapped within the interval of $[-\pi, \pi]$, it needs to be unwrapped before the estimation of height information. However, the presence of phase noise not only interferes with the phase unwrapping process, but it also affects the quality of topographic height information obtained from the interferogram. From the nature of the data, it is clear that fringes (lines of discontinuity due to phase wrapping) in the data should not be affected, which makes simple linear low-pass filtering techniques ineffective.

Several techniques have been proposed in the literature to reduce interferometric phase noise. The Lee filter, used for SAR images has been adjusted to filter out noise in InSAR images [2]. This filter makes use of directional windows to capture locally homogenous areas within which local statistics-based filtering is performed. While the Goldstein [3] and the modified Goldstein filters [4] employ a frequency domain approach to this problem. Recent techniques also use the wavelet transform [5] and fuzzy logic [6] in order to achieve the desired noise reduction in InSAR images. Work has also been done by the authors on a nonlinear two-stage filter structure that decomposes the interferogram into rough and smooth components, filters them independently, and combines them again [7]. An adaptive median filter developed as the first stage for that technique has been used as a noise estimator here.

This paper proposes a technique for noise reduction by selective weighting of the wavelet coefficients of the noisy image. In order to obtain estimates of noise content in each subband, a reference image is first generated by using a technique described in Section 2. An undecimated wavelet transform is used to decompose both the reference and the noisy interferograms, and the mean square error between the corresponding subband images of these two interferograms is taken as a measure of the noise present in that subband. The use of undecimated wavelet transform makes the image translation invariant [8] and prevents arbitrary disappearance of wavelet coefficients generated by image discontinuities. Since the interferometric phase is wrapped in the interval $[-\pi, \pi]$ all the computation is performed in the complex domain. The advantage of this technique over the one described in [7] and conventional

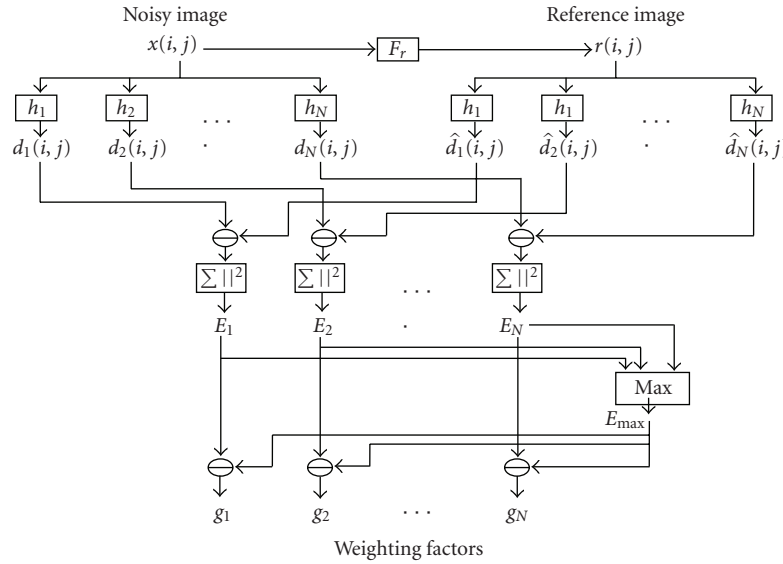

Figure 1: Weighting factor computation.

techniques based on the boxcar filter is that the proposed technique does not make the assumption that noise affects only the high-frequency components. It also provides a framework within which any nonlinear noise estimator can be incorporated.

2. NOISE ESTIMATOR

2.1. Reference image

The estimation of the noise content in each subband of the interferogram is important in computing the scaling factors. A nonlinear filter is used to generate a reference image, which is compared to the interferogram to estimate the relative noise distribution among the subbands. The reference image (for want of a better term) is used only to estimate the relative noise content in each subband and is not involved in any error minimisation technique. Hence, the quality of the output is not limited by the quality of the reference image. Here, a reference image is generated by a pivoting median filter with a variable window size that adapts to the local signal statistics, which is described in [7]. While any nonlinear filter whose response depends on the data can be used in place, the median filter was chosen due to its ease of implementation and its ability to preserve edges. In support of our choice, we have compared the performance of the technique using the median filtered image to that when using the actual noise-free image for a simulated interferogram and found they were almost identical (refer to Section 3). The lack of a noise-free image in a real case restricts this comparison to a simulated interferogram. Also, a pivoting median filter was chosen over a simple median filter as it takes into account the discontinuities introduced at odd multiples of π in the wrapped phase [9].

2.2. Weighting factor computation

An undecimated wavelet transform [10] is used to decompose the noisy image into N subband images with L levels of decomposition ($N = 3L + 1$). Each subband image is selectively weighted based on its noise content such that those with relatively low-noise content are weighted more than those with higher noise content. To estimate the relative noise content in them, the subband images of the noisy interferogram are compared to the corresponding subband images of the reference interferogram (Figure 1). This reference image $r(i, j)$ is obtained by passing the noisy image, $x(i, j)$ through a nonlinear filter, F_r:

$$r(i, j) = F_r\{x(i, j)\}. \tag{1}$$

Both the noisy and reference images are decomposed into N subband images using identical undecimated wavelet transforms. If we use $h_n(i, j)$ to denote the filter response that generates the nth subband image,

$$\begin{aligned} d_n(i, j) &= H_n\{x(i, j)\} = \sum_k \sum_l h_n(k, l)x(i - k, j - l), \\ \hat{d}_n(i, j) &= H_n\{r(i, j)\} = \sum_k \sum_l h_n(k, l)r(i - k, j - l), \end{aligned} \tag{2}$$

where d_n is the nth subband image of the noisy interferogram and $\hat{d}_n$ is the nth subband image of the reference interferogram.

Corresponding subband images are compared and the mean square error per pixel, E_n in each subband is computed.

$$E_n = \frac{1}{(P \times Q)} \sum_i \sum_j \left[d_n(i, j) - \hat{d}_n(i, j)\right]^2, \tag{3}$$

where, $P \times Q$ is the number of pixels in the image.

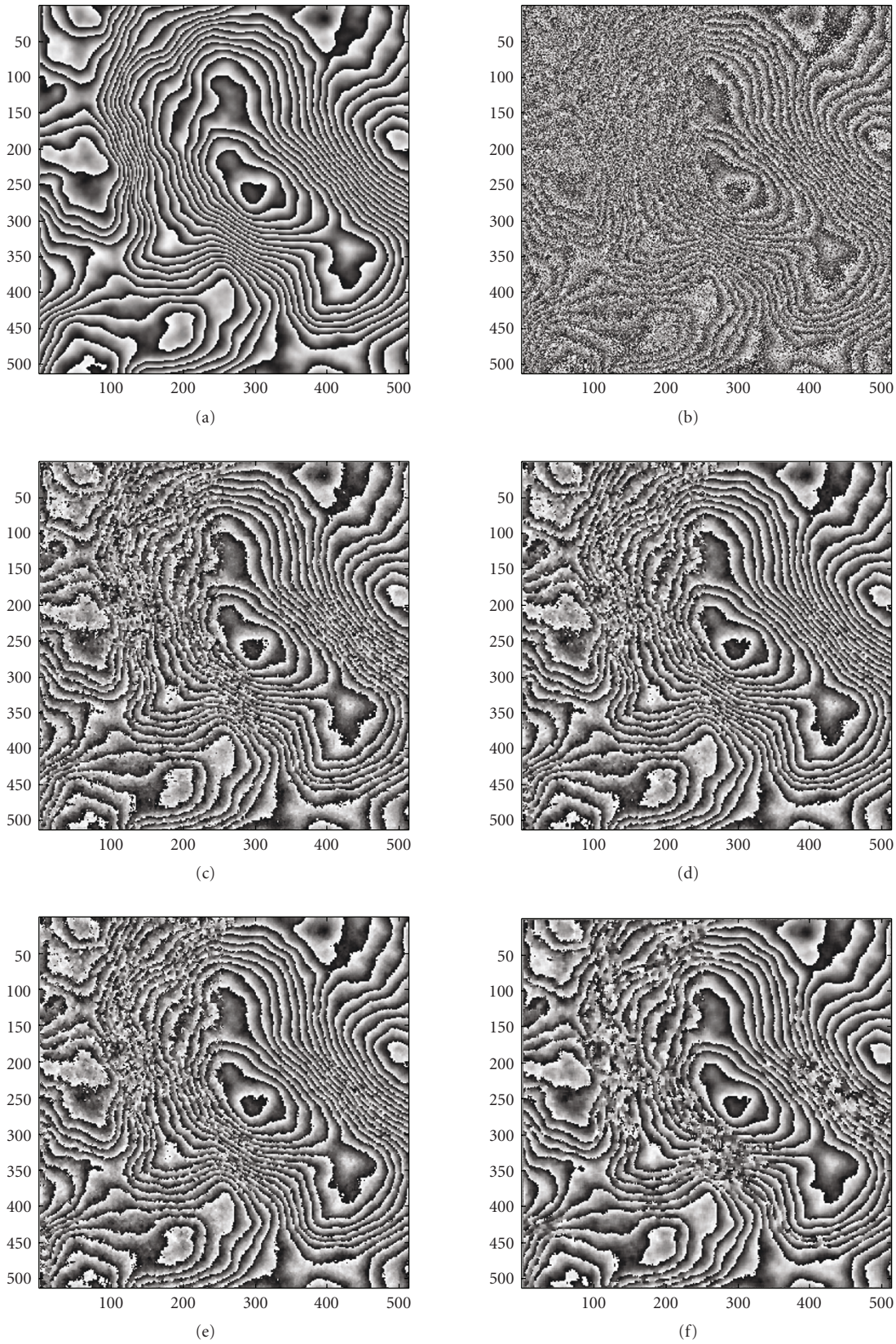

Figure 2: Filtered images obtained from simulated interferogram: (a) original wrapped phase image (512×512), (b) noisy interferogram with coherence values 0.2, 0.4, 0.6, and 0.8, counter clockwise from top left quadrant, (c) median filtered image (reference), (d) output of proposed filter, (e) proposed filter using (a) as reference, (f) boxcar filtered image.

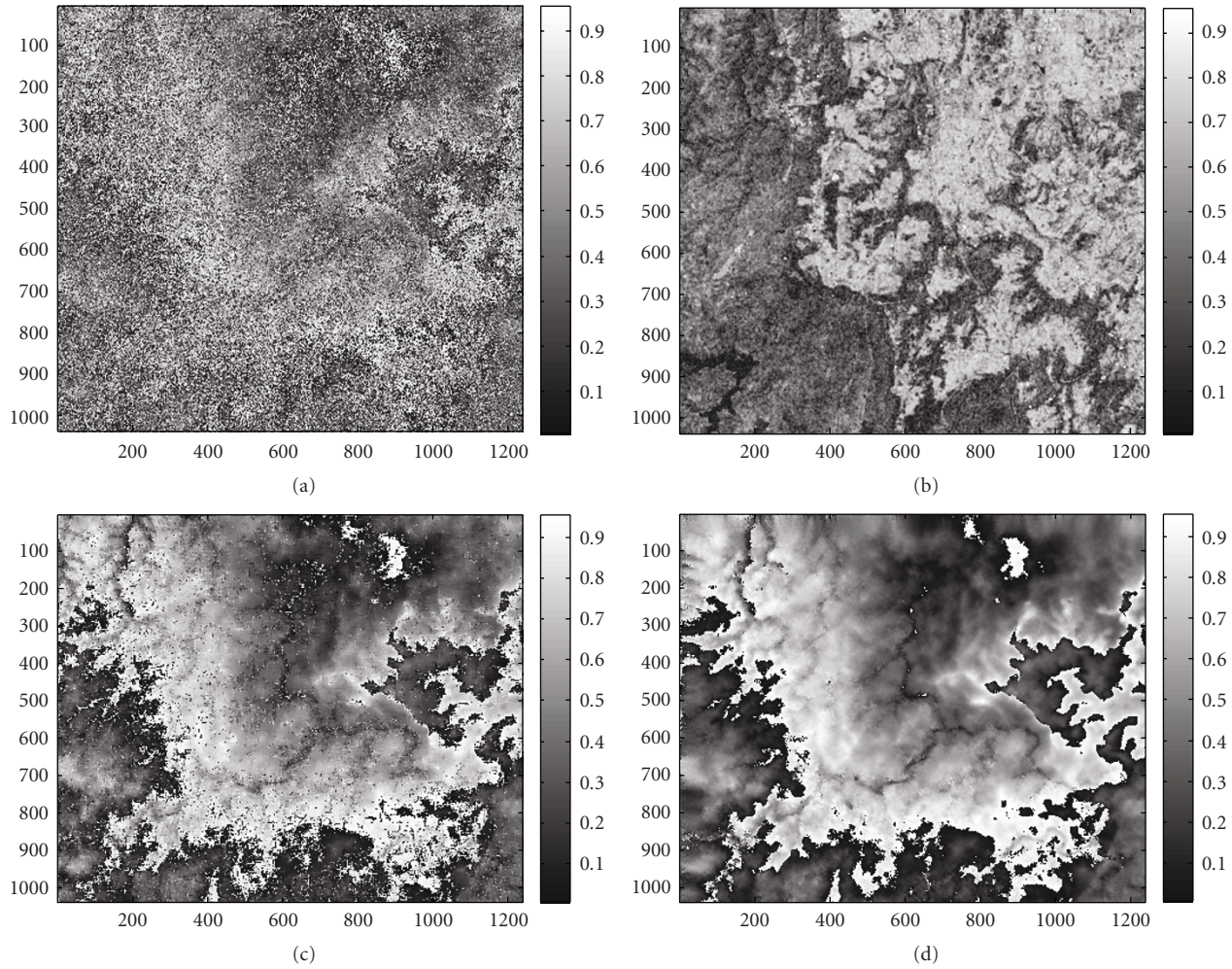

Figure 3: (a) Topographic fringes of an area over Appin, Australia from ERS-1/2 tandem mission: original interferogram (1037×1238), (b) coherence map corresponding to the interferogram, (c) median filtered interferogram—used as the reference image, (d) filtered image using proposed technique.

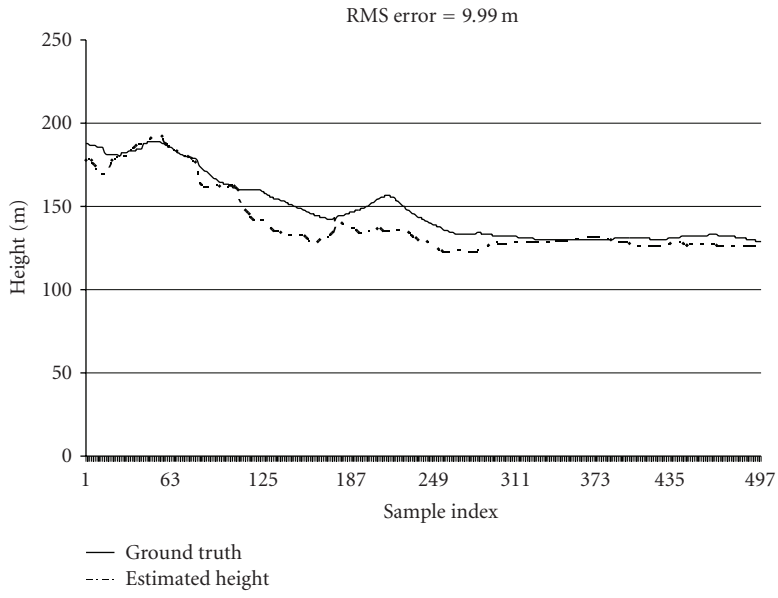

Figure 4: Height estimate from selective weighting technique (Route 1).

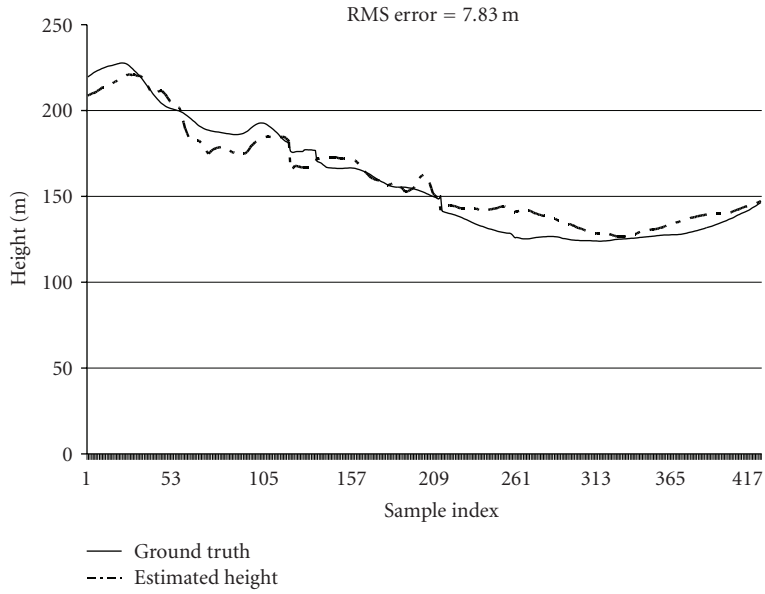

Figure 5: Height estimate from selective weighting technique (Route 2).

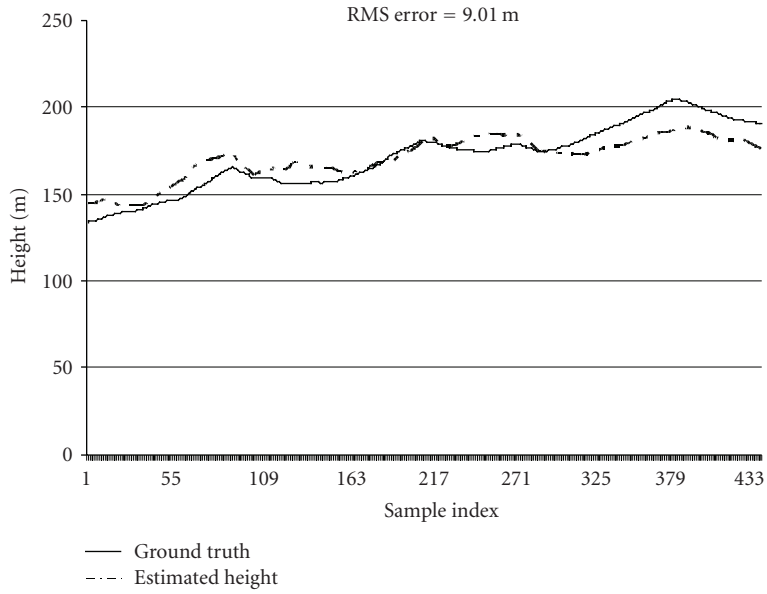

Figure 6: Height estimate from selective weighting technique (Route 3).

Comparing the mean square errors of each subband (E_n) to the largest mean square error ($E_{\max}$) gives us the weighting factor for that subband (g_n) which is inversely proportional to the noise content in that band.

$$E_{\max} = \max[E_1, E_2, \ldots, E_N],$$
$$g_n = E_{\max} - \sigma E_n \quad 0 \leq \sigma \leq 1. \tag{4}$$

where, σ is a constant that provides a trade-off between the amount of noise removed and any distortion that may be caused by over estimating the noise.

The wavelet decomposition filters are normalised such that they have unity pass band gain operate on wrapped phase image (each pixel lies in the range $[-\pi, \pi]$). Consequently, the mean square error per pixel is constrained to the range $[0, 4\pi^2]$. This in turn imposes an upper bound of $4\pi^2$ for the individual subband weighting factors. Setting σ to a value less than 1 will also prevent the theoretical possibility of the weighting factors from going to zero when the noise estimates in all the subbands are equal and thus not producing an image after wavelet reconstruction. However, this possibility will occur only when the noise estimation filter used to produce the reference image removes the same amount of noise from each subband, and thereby acting as an all-pass filter. In the work reported in this paper, a pivoting median filter was used to obtain the reference image, which

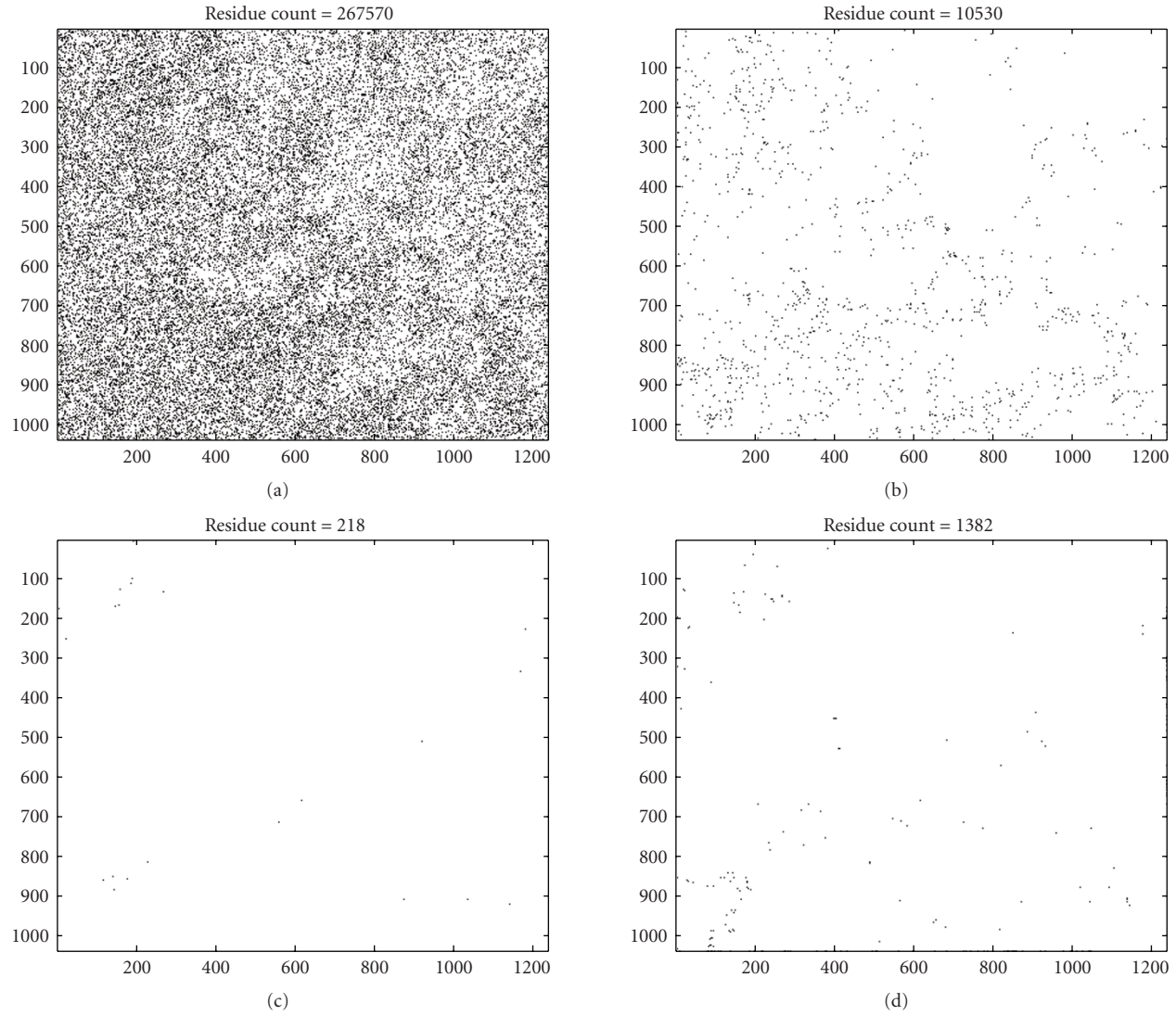

Figure 7: Residues of the interferograms: (a) original, (b) reference (median filtered), (c) output of proposed filter, (d) 11×11 boxcar filtered.

never acted as an-all pass filter and thus a value of 1 was used for σ.

When the change induced by the nonlinear filter (used to generate the reference image) in the nth subband is large, the mean square error E_n is large and consequently g_n is small. Conversely, if the change is small, E_n is small and g_n is large. Since subband coefficients with a large gain contribute more to the reconstructed image than those with a smaller gain, subbands which contain less noise and consequently are affected by the nonlinear filter to a lesser degree contribute more to the final image. The nonlinear filter thus acts as a noise estimator which determines the relative distribution of noise among the subbands, while noise reduction is carried out by wavelet reconstruction using weighted coefficients. This lends support to our argument that it is the ability of the nonlinear filter to identify noise rather than its denoising performance (the quality of the reference image) that is important. Also in support of this argument we have shown in Section 3, for a simulated image (where the actual noise-free image is available for comparison) the mean-squared error of the image produced by the proposed technique is smaller than that of the reference image used in the procedure.

3. EXPERIMENTAL RESULTS

3.1. Simulated InSAR phase images

The performance of the proposed technique was evaluated using both real and simulated data. The MATLAB toolbox for InSAR (Version 1.3) [11] was used to simulate an interferogram and the mean square error (MSE) of the output taken as a measure of performance. The use of simulated data also allowed us to test the technique on images with dense fringes and it was found that the technique preserved fringes well. The noisy interferogram with coherence values 0.2, 0.4,

Table 1: Root mean square (RMS) error comparison for simulated images.

Filter	RMSE for varying coherence (ρ), rad/sample				
ρ =	0.2	0.4	0.6	0.8	Avg
Noisy image	1.54	1.37	1.23	1.08	1.31
Boxcar	1.03	0.70	0.70	0.52	0.74
Median (reference)	1.08	0.72	0.62	0.48	0.73
Proposed filter	0.97	0.62	0.45	0.33	0.59
Proposed filter with noise-free image as reference	0.98	0.63	0.47	0.35	0.61

Table 2: Average root mean square (RMS) error comparison.

	Average RMS error			
	Proposed filter	Boxcar filter (11×11 window)	Lee filter [2]	Selective weighting filter [12]
Route 1	9.99 m	12.37 m	12.70 m	9.94 m
Route 2	7.83 m	10.14 m	11.13 m	8.38 m
Route 3	9.01 m	9.69 m	8.97 m	8.27 m

0.6, and 0.8 in each of its quadrants was filtered using the proposed technique and a boxcar filter. The image was also denoised using the actual noise-free image as the reference image. Figure 2 shows these images along with the median filtered image while Table 1 lists their mean square errors.

3.2. True InSAR phase images

The real data used for testing was an image of an area over Appin , Australia obtained from the ERS-1/2 tandem mission (Figure 3). The coherence map was estimated on a 12×12 window for the 4-look complex interferogram. Once filtered, the interferometric phase was unwrapped and a DEM generated from it using the EV-InSAR software. Height information obtained from this DEM along a few series of points (routes) was compared to the actual heights of the corresponding points in the surveyed area. The average root mean square error per point is then computed and taken as a measure of the filter's performance for comparison with the boxcar filter. Plots comparing the estimated and actual height profiles along the three routes are also included to show that the technique does not produce any localised large errors.

Table 2 lists the average root mean square error per point, while Figures 4, 5, and 6 show the height profiles along three routes over the surveyed area in Appin while using different filters for noise reduction.

Residues are local errors in the wrapped phase values encountered during the phase unwrapping process which follows noise reduction. Although the total elimination of residues is the ideal result of noise reduction, it is rarely achieved in practice. A reduction in their number is a valuable result, leading to a reduction in the complexity of the phase unwrapping processing. An analysis of residues was carried out on the Appin interferograms which indicates that the proposed technique results in a lower residue count when compared with boxcar filtering. Plots giving the location of the residues in the original, reference, and the filtered interferograms are included (Figure 7). These plots indicate that the density of residues is inversely related to coherence, with high coherence areas being practically free of residues while low coherence areas exhibiting a drastic reduction in the number of residues.

4. CONCLUDING REMARKS

A novel method for weighting the wavelet coefficients to reduce noise in SAR interferometric phase images has been proposed. A reference image generated by some other technique is used to estimate the noise content in each subband and consequently determine the weights for those subbands. The performance of the proposed technique is not limited by the filter used to generate the reference image and the quality of the denoised interferogram is superior to the quality of the reference interferogram. The technique is very effective in filtering out noise and reducing the number of residues while preserving the fringes in the interferogram. Moreover, the proposed technique is not optimised for a particular signal and/or noise model. Hence, performance is dependant only on the local signal-to-noise ratio.

ACKNOWLEDGMENT

This research work was supported by The Cooperative Research Centre for Spatial Information through Project 4.2 [13], whose activities are funded by the Australian Commonwealth's Cooperative Research Centre programme.

REFERENCES

[1] R. Bamler and P. Hartl, Synthetic aperture radar interferometry, *Inverse Problems*, vol. 14, no. 4, pp. R1R54, 1998.

[2] J.-S. Lee, K. P. Papathanassiou, T. L. Ainsworth, M. R. Grunes, and A. Reigber, A new technique for noise filtering of SAR interferometric phase images, *IEEE Transactions on Geoscience and Remote Sensing*, vol. 36, no. 5, part 1, pp. 14561465, 1998.

[3] R. Goldstein and C. Werner, Radar ice motion interferometry, in *Proceedings of the 3rd ERS Symposium*, pp. 969970, Florence, Italy, March 1997.

[4] I. Baran, M. P. Stewart, B. M. Kampes, Z. Perski, and P. Lilly, A modification to the goldstein radar interferogram filter, *IEEE Transactions on Geoscience and Remote Sensing*, vol. 41, no. 9, part 2, pp. 21142118, 2003.

[5] C. López-Martínez and X. Fàbregas, Modeling and reduction of SAR interferometric phase noise in the wavelet domain, *IEEE Transactions on Geoscience and Remote Sensing*, vol. 40, no. 12, pp. 25532566, 2002.

[6] B. Aiazzi, S. Baronti, M. Bianchini, A. Mori, and L. Alparone, Filtering of interferometric SAR phase images as a fuzzy matching-pursuit blind estimation, *EURASIP Journal on Applied Signal Processing*, vol. 2005, no. 20, pp. 32203230, 2005.

[7] D. Meng, V. Sethu, E. Ambikairajah, and L. Ge, A novel technique for noise reduction in InSAR images, *IEEE Geoscience and Remote Sensing Letters*, vol. 4, no. 2, pp. 226230, 2007.

[8] G. Beylkin, On the representation of operators in bases of compactly supported wavelets, *SIAM Journal on Numerical Analysis*, vol. 29, no. 6, pp. 17161740, 1992.

[9] T. Zhi, L. Jingwen, and Z. Yinqing, Analysis on noise reduction method for interferometric SAR image, in *Proceedings of IEEE International Geoscience and Remote Sensing Symposium (IGARSS '04)*, vol. 6, pp. 42434246, Anchorage, Alaska, USA, September 2004.

[10] P. Dutilleux, An implementation of the 'algorithme a trous' to compute the wavelet transform, in *Wavelets: Time-Frequency Methods and Phase Space*, Inverse Problems and Theoretical Imaging, pp. 298304, Springer, Berlin, Germany, 1989.

[11] B. Kampes and S. Usai, Doris: the delft object-oriented radar interferometric software, in *Proceedings of the 2nd International Symposium on Operationalization of Remote Sensing (ORS '99)*, pp. 14, ITC, Enschede, The Netherlands, August 1999.

[12] V. Sethu, E. Ambikairajah, and L. Ge, Noise reduction in SAR interferograms using undecimated wavelet transform, in *Proceedings of the 2nd International Symposium on Geo-Information for Disaster Management*, Goa, India, September 2006.

[13] The CRC-SI Project 4.2, 2006, http://www.crcsi.com.au/pages/project.aspx?projectid=72.